

# Thermal Transport across a Continuous Metal-Insulator Transition

P. Haldar, M. S. Laad and S. R. Hassan

*Institute of Mathematical Sciences,  
Taramani, Chennai 600113, India*  
and

*Homi Bhabha National Institute Training School Complex,  
Anushakti Nagar, Mumbai 400085, India*

(Dated: February 10, 2017)

The celebrated Wiedemann-Franz (WF) law is believed to be robust in metals as long as interactions between electrons preserve their fermion-quasiparticle character. We study thermal transport and the fate of the WF law close to a continuous metal-insulator transition (MIT) in the Falicov-Kimball model (FKM) using cluster-dynamical mean-field theory (CDMFT). Surprisingly, as for electrical transport, we find robust and novel quantum critical scaling in thermal transport across the MIT. We unearth the deeper reasons for these novel findings in terms of (i) the specific structure of *energy-current* correlations for the FKM and (ii) the microscopic electronic processes which facilitate energy transport while simultaneously blocking charge transport close to the MIT. However, within (C)DMFT, we also find that the WF law survives at  $T \rightarrow 0$  in the incoherent metal right up to the MIT, even in absence of Landau quasiparticles.

PACS numbers: 74.25.Jb, 71.27.+a, 74.70.-b

In normal metals at low temperature  $T$ , the celebrated Wiedemann-Franz law [1] relates the electrical and thermal conductivities via a universal Lorenz number,  $L_0 = \frac{K_{el}(T)}{T\sigma_{xx}(T)} = \frac{\pi^2 k_B^2}{3e^2}$ , the Sommerfeld value. Even in strongly correlated metals [2], the WF law still holds as  $T \rightarrow 0$  as long as the metallic state is a LFL, presumably due to a Ward identity [3]. Explicit counter-examples are  $D = 1$  Luttinger liquids [4], cuprates [5] and  $f$ -electron systems [6] near quantum phase transitions, where Landau quasiparticle views break down. It is well known that Landau quasiparticle picture also naturally breaks down at interaction- or disorder-driven metal-insulator transitions (MIT) (at  $T = 0$ ). However, the former are generically first-order, and are accompanied by instabilities to more conventional symmetry-broken states at lower  $T$ , preventing clean study of the breakdown of the WF law. Thus, continuous MITs at  $T = 0$  turn out to be an ideal playground to study this issue.

Quite generally, quantum critical fluctuations at a continuous MIT affect critical features in conductivity. This has been studied in the context of the finite-but low  $T$  critical end-point in the  $d = \infty$  Hubbard model [7], and recent CDMFT work for the FKM also shows that conductivity [8] and magneto-transport [9] exhibit remarkable quantum-critical scaling at a “Mott” QCP. Whether and how such novel QC features show up in thermal transport is a very interesting, albeit scarcely studied, issue. Thermal transport primarily measures *energy current* correlations in solids [10]. Most generally, the electronic contribution to the thermopower,  $S_{el}(T)$ , is best interpreted as the entropy of an electric current [11]. In weakly correlated metals,  $S_{el}(T) \simeq A_1 T$  is small at low  $T$ . In strongly correlated Landau Fermi Liquid (LFL) metals, in contrast,  $S_{el}(T) = AT$  is sizably enhanced at low  $T$ , passes through a broad maximum at inter-

mediate  $T$  before asymptoting to the Heikes law at high  $T \gg T_{LFL} \simeq t_{eff} = z_{FL} t$ , where  $t_{eff}$  is the correlation-induced reduction of the bare kinetic energy ( $t$ ) and  $z_{FL}$  is the Landau quasiparticle residue. In the Mott insulator, one expects  $S_{el}(T \rightarrow 0)$  to diverge owing to the loss of carriers upon gap opening. It is then natural to expect that soft quantum-critical fluctuations at a QCP associated with a continuous MIT should also reflect in thermal transport.

Here, we study thermal transport in the simplest lattice model of interacting fermions, the Falicov-Kimball model (FKM) in detail within a two-site cluster-DMFT [10] within the alloy-analogy formalism. Specifically, we (i) unearth quantum-critical scaling in thermal transport and correlate it with electrical transport, and (ii) examine the microscopic origin of the electronic processes involving energy current which distinguish thermal from electrical transport. The FKM is ideal since it shows a continuous “Mott” MIT within both DMFT [12] and CDMFT [13, 14]. We focus on quantum critical features in thermal transport in the strong-scattering regime where  $k_F l \simeq 1$  invalidates quasiclassical Boltzmann approaches, since the very concept of well-defined LFL quasiparticles breaks down.

As for the conductivity tensor [9], it turns out that thermal transport co-efficients can be precisely evaluated within our two-site CDMFT [14]. This is because the irreducible cluster resolved particle-hole vertex corrections rigorously drop out from the Bethe-Salpeter equations (BSE) for all current-current correlation functions [15]. Further, having explicit closed-form analytical expressions for the cluster propagators,  $G(\mathbf{K}, \omega)$ , minimizes the computational cost, even within CDMFT. We detail the computational scheme (exact-to- $O(1/d)$ ) in **SI1**.

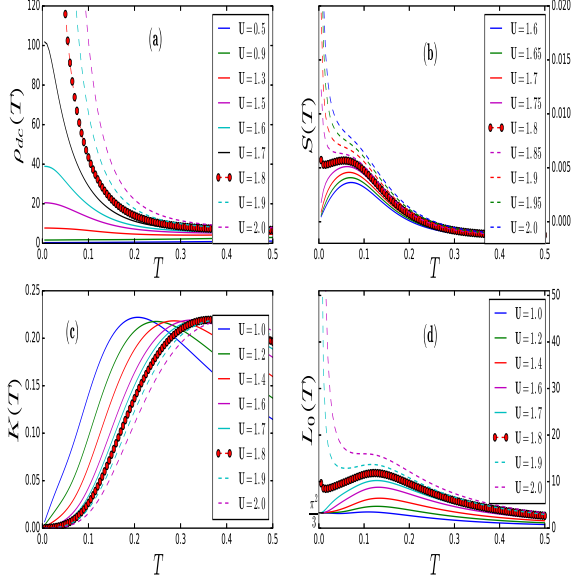


FIG. 1: (Color online)  $dc$  resistivity  $\rho_{dc}(T)$  (a), thermopower  $S_{el}(T)$  (b), thermal conductivity  $K_{el}(T)$  (c) and Lorenz number  $L_0(T)$  (d) for the FKM as functions of  $U$ . At the Mott QCP (bold red circles) at  $U_c = 1.8$ , both  $S_{el}(T)$ ,  $L_0(T)$  attain finite values, cleanly separating metallic and insulating behavior. Concomitantly,  $\rho_{dc}(T \rightarrow 0)$  diverges and  $K_{el}(T) \simeq T^{1+\nu}$  with  $\nu \simeq 4/3$  [8].

## RESULTS

Consider non-interacting electrons half-bandwidth as unity. Since we aim to correlate specific features in electrical and thermal transport with each other, we start by recapitulating  $dc$  resistivity. In Fig. 1(a), we exhibit the  $dc$  resistivity,  $\rho_{dc}(U, T)$  as a function of  $U$  as the system is driven through a continuous MIT at  $U_c = 1.8$  [8]. It is clear that at intermediate  $0.95 < U < 1.8$ , clear pseudogap signatures appear in  $\rho_{dc}(T)$  over a progressively wider  $T$ -range, between the high- $T$  incoherent metal and a low- $T$  very bad metal, before the MIT occurs for  $U \geq 1.8$ . This feature is associated with proximity to the “Mott” quantum critical point (QCP) occurring between a  $T = 0$  very bad metal and a “Mott” insulator at  $U_c$ . We are interested in how this Mott quantum criticality manifests in thermal transport.

In Fig. 1(b), we show how the electronic contribution to the thermopower varies across the continuous MIT. Several features stand out: (i) for weak-to-intermediate  $U < 0.9$ ,  $S_{el}(T) \simeq AT$  at low  $T < 0.025t$  is small (not shown), as expected for a weakly correlated metal, and goes hand-in-hand with  $\rho_{dc}(T) \simeq \text{const}$  at low  $T$ . (ii) In the intermediate-to-strong coupling ( $0.9 < U < 1.7$ ) regime, where one is in the increasingly bad-metallic low- $T$  regime,  $S_{el}(T)$  is still linear-in- $T$ , but is significantly

enhanced by factors of  $O(50 - 100)$  over its weakly correlated values.  $S_{el}(T)$  also exhibits a broad peak around  $T^* \simeq 0.04t$ , before continuously falling off to achieve the Heikes value at very high  $T$ . It is very interesting that  $S_{el}(U, T) = A(U)T$  with  $A(U)$  increasing with  $U$  holds throughout this very bad metallic regime, even as  $\rho_{dc}(T \rightarrow 0) \simeq 100\hbar/e^2$ . This is the regime in which no quasiclassical Boltzmann view of transport is tenable, since application of Drude-Boltzmann ideas would necessarily yield  $k_F l < 1$  (where no  $1/k_F l$ -expansion is possible). Since thermopower features result solely from a non-Landau quasiparticle cluster propagator within CDMFT, this implies that this low- $T$  enhancement in  $S_{el}(T)$  involves non-Landau-FL quasiparticle (branch-cut continuum) excitations. Just before the MIT,  $S_{el}(T \rightarrow 0)$  is still linear in  $T$ , but is enhanced by a factor of about 100 relative to its small  $U$  value. (iii) Finally, precisely at the QCP  $U = 1.8$ , clear anomalies obtain:  $S_{el}(T)$  increases with decreasing  $T$  right down to  $T \rightarrow 0$ , but achieves a *finite* value. For  $U > 1.8$ , opening of the “Mott” gap in the one-electron density-of-states [14] produces a divergent  $S_{el}(T \rightarrow 0)$ . This is not a violation of the Nernst theorem, since  $\rho_{dc}(T \rightarrow 0)$  simultaneously diverges.

It is clear from Fig. 1(b) that  $S_{el}(U, T \rightarrow 0)$  curves fan out to either metallic or insulating values, except at the “Mott” QCP, where  $S_{el}$  is finite. This suggests that, like electrical transport [8], thermal transport should also exhibit characteristic quantum critical features. To unravel this novel possibility, we repeat earlier procedure [8] for thermopower by making the metallic and insulating curves fall on to two “universal” curves by scaling both with a  $U$ -dependent scale,  $T_0^{th}(U)$ . In Fig. 2(a), we exhibit  $\log(S_{el}(T)/S_{el}^{(c)})$  versus  $T$ . Remarkably, this bares clear signatures of “mirror” symmetry, exactly as in electrical transport. This strongly presages novel “Mott” quantum critical features in thermal transport as well. More clinching support for such criticality is seen in Fig. 2(b), where we show  $\log(S_{el}(T)/S_{el}^{(c)})$  versus  $T/T_0^{th}(U)$  as done earlier [8]. Remarkably, we find (i) clear “mirror” symmetry between metallic and insulating curves around the critical  $S_{el}(U_c)$ , and (ii)  $T_0^{th}(\delta U) = c_{th}|\delta U|^\eta$  with  $\eta = 1$  (in Fig. 2(c)). To further cement this unusual idea, we also show in Fig. 2(d) the “beta”-function (or the Gell-Mann Low function) for thermopower,  $\beta_{th}(s) = d[\log(s)]/d[\log(T)]$  versus  $s$ , with  $s = (S_{el}(T)/S_c(T))$  and  $S_c(T)$  being the critical thermopower right at the MIT (red circled curve in Fig. 1(b)). Remarkably, we find  $\beta_{th}(s) \simeq \log(s)$  near the MIT, exactly as found before for the  $dc$  conductivity. This conclusively establishes novel quantum-critical scaling of the thermopower at the “strong localization” MIT as well.

Appearance of such quantum-critical scaling in thermopower at the MIT is very surprising, and calls for deeper analysis. Since  $S_{el}(T)$  measures “mixed” elec-

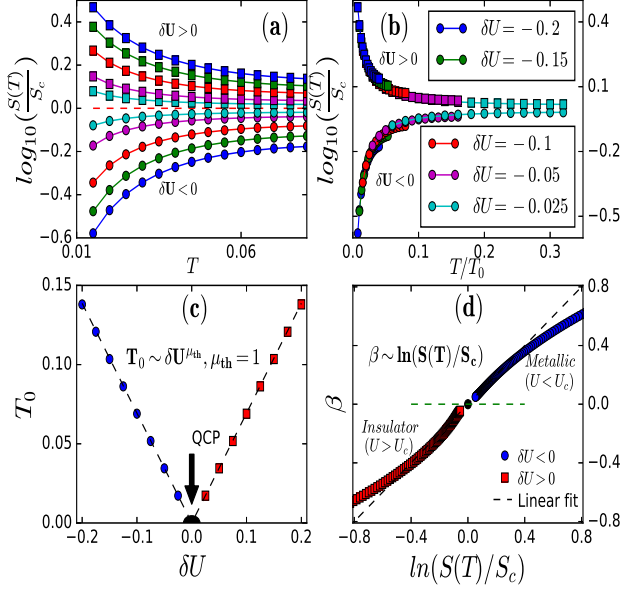


FIG. 2: (Color online) Mott Quantum critical scaling in thermopower  $S_{el}(U, T)$  across the MIT.  $\log(S_{el}(T)/S_c)$  vs  $T$  exhibits almost perfect “mirror symmetry” around  $U_c$  (panel (a)). Collapse of metallic and insulating curves onto two “universal” curves upon scaling (panel (b)).  $T_0^{th}(\delta U) = c|\delta U|^{\mu_{th}}$  with  $\mu_{th} = 1$  (panel (c)). The “beta function” varies like  $\beta(s) \simeq \log(s)$  with  $s = S_{el}(T)/S_c$  close to the MIT and is continuous across  $U_c$  (panel (d)). This is evidence that Mott quantum critical scaling in electrical transport [8] extends to thermal transport as well.

trical current-energy current correlations, these features must originate from long-time behavior of  $\langle j_e(\tau)j_Q(0) \rangle$ . Let us look more closely at this term. The energy current, in contrast to the electrical current, involves *three* sites, and reads [16]

$$j_{i,Q} = t^2 (ic_{i-\delta}^\dagger c_{i+\delta} + h.c.) - \frac{U}{2} (j_{i-\delta,i} + j_{i,i+\delta}) (n_{i,d} - \frac{1}{2}) \quad (1)$$

where we have relabelled  $c \rightarrow c_\uparrow, d \rightarrow c_\downarrow$ ,  $\delta$  denotes nearest neighbors of site  $i$ , and  $j_{i,i+\delta}$  is the electrical current operator. For the FKM, we have  $[n_{i,d}, H] = 0$  for all  $i$ , and thus  $n_{i,d} = 0, 1$  only. The expression for  $j_{i,Q}$  now simplifies to a revealing form

$$j_{i,Q} = t^2 (ic_{i-\delta}^\dagger c_{i+\delta} + h.c.) \pm \frac{U}{4} (j_{i-\delta,i} + j_{i,i+\delta}) \quad (2)$$

for  $(+, -)$  corresponding to  $n_{i,d} = 0, 1$ . Thus, for the FKM, we find that  $j_{i,Q}$  is directly related to the electrical current operator, providing direct insight into the underlying reason for emergence of very similar quantum critical scaling responses in  $\rho_{dc}(T)$  [8] and  $S_{el}(T)$  above. Simply put, energy current correlations mirror those of the electrical current.

Armed with these positive features, we now study the electronic contribution to the thermal conductivity,  $K_{el}(T)$ , in Fig. 1(c). In the small  $U$  regime,  $K_{el}(T) \simeq A_2 T$  is linear in  $T$ , as would be expected for a weakly correlated metal, with transport being determined by a LFL of “dirty” quasiparticles. This is the regime where  $\rho_{dc}(T \rightarrow 0) \simeq const$ , and formally corresponds to the weak scattering regime where  $k_F l \gg 1$  holds (this is thus the regime where self-consistent Born approximation (SCBA) applies). As we enter the intermediate-to-strong scattering regime with  $0.95 < U < 1.8$ , progressive bad metallicity in resistivity goes hand-in-hand with emergence of a low-energy scale in  $K_{el}(T)$ , where its power-law-in- $T$  ( $K_{el}(T) \simeq T^n, n > 1$ ) behaviour at intermediate- $T$  crosses over to a linear-in- $T$  variation as  $T \rightarrow 0$ . Precisely at  $U_c = 1.8$ , we find  $K_{el}(T) \simeq T^{1+\nu}$ . This behavior is characteristic of heat conductivity arising from non-fermionic excitations. In our case, such collective modes can only be of electronic origin: these are the low-energy particle-hole fluctuations, which remain low-energy excitations in the insulator when charge degrees of freedom are frozen out at low energies. Upon closer inspection, we see that the linear-in- $T$  contribution gives way to a power-law behavior ( $K_{el}(T) \simeq T^{1+\nu}, 0 < \nu < 1$ ) right down to  $T = 0$  for  $U = 1.8$  within our numeric, *precisely* where the MIT occurs. This finding is completely consistent with breakdown of the LFL quasiparticle description in the quantum critical region associated with the MIT.

Even more insight into the breakdown of the LFL quasiparticle description close to the MIT is provided by examination of the  $T$ -dependent Lorenz number,  $L_0(T) = K_{el}(T)/T\sigma_{xx}(T)$ , as a function of  $U$ . In Fig. 1(d), we exhibit  $L_0(U, T)$  across the MIT. Throughout the metallic phase, including the very bad metal,  $L_0(T \rightarrow 0) = \frac{\pi^2}{3}$  (in units of  $k_B = 1 = e$ ), even though  $L_0(T)$  exhibits significant  $T$ -dependence up to the lowest  $T$ , especially for  $U > 1.4$ , implying no breakdown of the WF law in the metallic phase. Precisely at the MIT, however,  $L_0(T \rightarrow 0) \simeq 10$ , indicating breakdown of the WF law exactly at the MIT. In the insulator ( $U > 1.8$ ),  $L_0(T \rightarrow 0)$  diverges, as it must, since  $K_{el}(T) \simeq T^3$  while  $\rho_{dc}(T) \simeq \exp(E_g/k_B T)$ . Our finding is remarkable because, whilst the resistivity shows clear precursor features of impending proximity to the MIT via progressive enhancement of bad-insulating and very bad metallic regimes beginning from  $U = 0.95$ , both  $S_{el}(T)$  and  $K_{el}(T)$  continue to display apparently conventional behavior right up to the MIT. Further, spectral responses clearly show non-Landau-FL metallicity [14], and while one may argue for a non-WF behavior at any  $T \neq 0$ , our results indicate no breakdown of the WF law at  $T = 0$ .

Remarkably, upon proper rescaling, it now turns out that  $\sigma_{xx}(T), S_{el}(T), K_{el}(T)$  and  $L_0(T)$  all exhibit clear quantum-critical scaling features. At the QCP, we find (not shown) that  $K_{el}(T) \simeq T^{7/3} = T^{1+\nu}$  with  $\nu =$

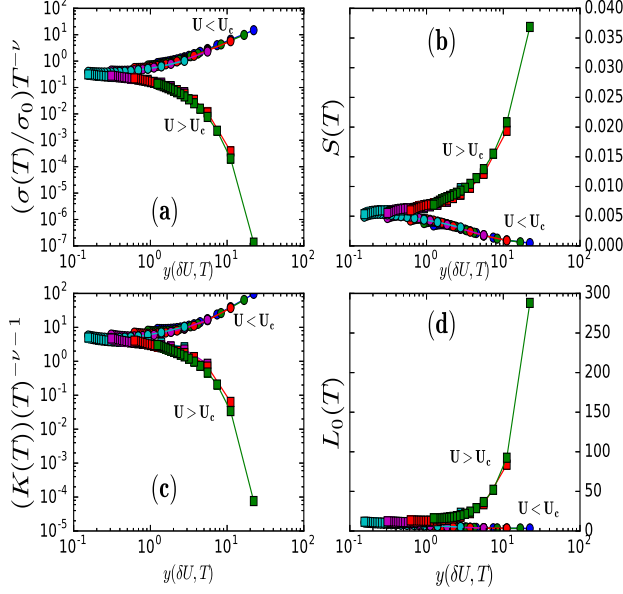


FIG. 3: (Color online) Quantum critical scaling in  $S_{el}(T)$  (panel (b)), Lorenz number (panel (d)), scaled electrical conductivity,  $T^{-\nu}\sigma_{dc}(T)$  (panel (a)) and scaled thermal conductivity,  $T^{-1-\nu}K_{el}(T)$  (panel (c)) when plotted as functions of the “scaling variable”  $y(U, T) = |U - U_c|/U_c T$ , demonstrating clean quantum critical scaling in electrical as well as thermal transport at the Mott QCP.

4/3. Recalling that  $\nu = 4/3$  is precisely the correlation length exponent we find for the  $dc$  conductivity [8], this suggests an alternative way to exhibit quantum critical scaling that bares the link between electrical and thermal transport. In Fig. 3, we find that  $T^{-4/3}\sigma_{xx}(T)/\sigma_0$ ,  $S_{el}(T)$ ,  $T^{-7/3}K_{el}(T)$  and  $L_0(T)$  exhibit clear collapse of the metallic and insulating curves onto two clear branches when plotted as a function of the “scaling variable”  $y = |U - U_c|/U_c T$ , *i.e.*, as a function of the distance from the “Mott” QCP. Since  $\sigma_{xx}(U) \simeq (U_c - U)^{4/3}$  as found earlier [8],  $\nu = 4/3$  and  $z = 1$ , as expected for the FKM. Further,  $z\nu = 4/3 > (2/d)$  implies that the Harris criterion holds, implying a genuinely *clean* QCP. Again, these features reflect the finding above, where energy current correlations simply mirror the electrical current correlations for the FKM, providing direct microscopic rationale for closely related quantum-critical transport in both. We are aware of only one previous study [17] where this issue was studied phenomenologically, by using the *experimental* conductivity as an input into the Kubo formula for the  $L_{lm}$ . In contrast, our results emerge from a truly microscopic CDMFT formulation for the FKM, and our finding of  $z = 1$  is very different from  $z = 3$  and  $\nu = 1$  (latter taken from experimental conductivity data). It is also different from  $z = d$  found [18, 19] for scaling in the non-interacting dis-

order model. Together with Mott-like criticality in transport [8], these differences reflect the qualitatively distinct “strong coupling” nature of the QCP in the FKM. In **SI2**, we show corresponding single-site DMFT results for thermal transport, and demonstrate that CDMFT performs much better than DMFT at pinpointing critical scaling features.

What is the microscopic origin of boson-like collective modes that can provide a distinct channel for heat conduction which simultaneously blocks charge transport? It is most instructive to invoke the analogy with the Hubbard model, where one-electron excitations in the Mott insulator are frozen out at low energies  $\omega < \Delta_{MH}$ , the Mott-Hubbard gap in the one-electron DOS. Were one to consider the Hubbard model, dynamical *bosonic* spin fluctuations, originating from second-order-in- $(t/U)$  virtual one-electron hopping processes, would be the natural low-energy excitations. However, in the FKM-like binary alloy model we consider, identifying  $c \rightarrow c_\uparrow$ ,  $d \rightarrow c_\downarrow$  leads to an Ising super-exchange to second order in a  $(t/U)$  expansion when  $U \gg t$  in the “Mott” insulator. It is important, exactly as in the Hubbard case, that it is the virtual hopping of a  $c$ -fermion between neighboring sites (from 0 to  $\alpha$  and back in our two-site cluster [14]) that is necessary to generate such a boson-like mode. Since this is *not* a real low energy charge fluctuation, it cannot cause real charge transport. But it does lead to a gain  $O(-t^2/U)$  in super-exchange energy; *i.e.*, energy is *not* conserved, and so these virtual charge fluctuations indeed cause energy transport. Physically, this n.n hopping in a gapped “Mott” insulator involves creation of a particle-hole pair (a holon-doublon composite on neighboring sites). At low energy, this local “exciton” is effectively a bosonic mode that disperses on the scale of  $J \simeq t^2/U$ . These bosons are thus *not* necessarily linked to any broken symmetry, but naturally emerge in a “Mott” insulator. In our CDMFT, the dynamical effects of such “excitonic” inter-site correlations on the cluster length scale *are* fed back into the cluster self-energy, and thus the basic process leading to energy transport but not charge transport *is* included in CDMFT. This is the underlying reason for the qualitative differences in electrical vis-a-vis thermal transport we observe above. It is also the reason (**SI2**) why CDMFT performs much better when we study quantum critical scaling in thermal transport. These “bosons” are thus natural candidates that can account for our finding of  $K_{el}(T) \simeq T^{1+\nu}$  in the proximity of the MIT.

Very interestingly, a series of careful experiments on two-dimensional electron gases (2DEGs) show remarkable features [22]: (i) in the low- $n_s$  regime where  $\rho \gg h/e^2$ , the activated  $T$ -dependence of  $\rho_{dc}(T)$  shows a remarkable “slowing down” to an extremely bad metallic state, even as  $\rho_{dc}(T \rightarrow 0) \simeq 250h/e^2$ , (ii) in the *same*  $n_s$ -regime, the thermopower shows hugely enhanced values (two orders of magnitude above the Mott value)



and, perhaps even more remarkably, exhibits linear-in- $T$  behavior reminiscent of normal metals precisely below 1.0 K. It may be possible to apply our high- $D$  approach, which focuses on short-ranged correlations, to these mesoscopic systems *if* one could model the system as a 2DEG influenced by strong scattering from atomic-sized (strong) scattering charged centers. In light of our calculations, the dichotomy between the  $T$ -dependence of  $\rho_{dc}(T)$  and  $S_{th}(T)$  can be interpreted as follows: a real charge excitation is blocked in the “strong-disorder” limit of the FKM near the MIT due to blocking effects associated with Mottness, explaining the extraordinarily high  $\rho_{dc}(T \rightarrow 0)$  below 1.0 K. But a collective particle-hole (or holon-doublon composite in Hubbard model lore) excitations are real low-energy electronic collective modes that naturally arise in this regime, and lead to a hugely enhanced  $S_{th}$ . It is interesting that our strong-coupling approach seems to rationalize the very unusual experimental observations in a single picture which emphasizes proximity to a (Mott-like) localization transition. That such observations maybe subtle manifestations of novel phase fluctuation effects is not inconsistent with our view either, since it follows directly from the number-phase uncertainty principle that increasing proximity to electronic localization will necessary generate large phase fluctuation-dominated state(s).

Clear quantum-critical scaling features in  $S_{el}(T)$ ,  $K_{el}(T)$  and  $L_0(T)$  at the MIT strongly testifies to robust quantum critical scaling of thermal transport at a continuous MIT. Ours is a truly microscopic approach, and is best valid in the strong localization regime ( $k_{Fl} \simeq 1$ ), where a Hubbard-like band-splitting type of MIT obtains. This is the limit opposite to the well-studied weak localization (WL) case, where a perturbative-in- $1/k_{Fl}$  expansion is possible: at strong localization, the criticality is better rationalized in terms of a locator expansion [21], and exhibits signatures expected of a continuous “Mott” quantum criticality. Moreover, we are also able to connect these critical features in a very transparent way to those observed in electrical conductivity by analyzing the structure of underlying correlations, thereby providing a direct rationalization for our findings. In view of the fact that the one-band Hubbard model exhibits “quantum critical” scaling in  $dc$  transport near the finite- but low  $T$  end-point of the line of first-order Mott transitions, it would also be interesting to study the possibility of related features in thermal transport for such cases in future if the finite- $T$  critical end-point of the Mott transition could be driven to sufficiently low  $T$ .

- [2] M. Tanatar *et al.*, Science, **316**, 1320 (2007).
- [3] C. Castellani *et al.*, Phys. Rev. B **37**, 9046 (1988).
- [4] C. L. Kane, Mathew P.A. Fisher, Phys. Rev. Lett. **68**, 8 (1992).
- [5] R. W. Hill *et al.*, Nature, Vol **414**, 711 (2001).
- [6] F. Steglich *et al.*, Journal of Low Temperature Physics, **99**, 3, pp 267-281 (1995).
- [7] H. Terletska *et al.*, Phys. Rev. Lett. **107**, 026401 (2011).
- [8] P. Haldar, M. S. Laad and S. R. Hassan, Phys. Rev. B **94**, 081115(R) (2016)
- [9] P. Haldar, M. S. Laad, S. R. Hassan, Madhavi Chand and Pratap Raychaudhuri, arXiv: 1603.00779.
- [10] J. K. Freericks *et al.*, Phys. Rev. B **64**, 245118 (2001); J. K. Freericks *et al.*, Phys. Rev. B **68**, 195120 (2003).
- [11] Maekawa, S., Tohyama, T., Barnes, S.E., Ishihara, S., Koshibae, W., Khaliullin, *Physics of Transition Metal Oxides, Springer Series in Solid-State Sciences*, G. (2004)
- [12] J. K. Freericks and V. Zlati, Rev. Mod. Phys. **75**, 1333 (2003).
- [13] M. Jarrell and H. R. Krishnamurthy, Phys. Rev. B **63**, 125102 (2001).
- [14] P. Haldar, M. S. Laad and S. R. Hassan, arXiv:1603.00301.
- [15] K. Haule and G. Kotliar, Europhys. Lett., **77**, 27007 (2007)
- [16] X. Zotos and P. Prelovsek, Phys. Rev. **B53**, 983 (1996)
- [17] C. Villagonzalo, R. A. Roemer, M. Schreiber, Ann. Phys. [Leipzig] **8**, Spec. Issue, SI-269 (1999).
- [18] F. Wegner, *Localization, Interaction and Transport Phenomena*, B. Kramer, G. Bergmann and Y. Bruynseraede, eds., *Springer Series in Solid-State Sciences*, vol. **61** (Springer, Berlin, 1985) p. 99.
- [19] T.R. Kirkpatrick, D. Belitz, arXiv:1602.01447.
- [20] F. Milde *et al.*, Phys. Rev. B **61**, 9 (2000)
- [21] V. Dobrosavljevi *et al.*, Phys. Rev. Lett. **79**, 455 (1997).
- [22] V. Narain *et al.*, Comptes Rendus Physique **17** (issue 10), 1123 (2016), and references therein.

---

[1] R. Franz, G. Wiedemann, Annalen der Physik (in German) **165** (8): 497531 (1853).

## SI1: General Formulation for Thermal Transport

In contrast to the electrical conductivity which involves the particle current,  $\mathbf{j}_e = \sum_{\mathbf{q}} \mathbf{v}_{\mathbf{q}} c_{\mathbf{q}}^\dagger c_{\mathbf{q}}$  with  $\mathbf{v}_{\mathbf{q}} = \nabla_{\mathbf{q}} \epsilon_{\mathbf{q}}$  for an unperturbed band structure  $\epsilon_{\mathbf{q}}$ , the heat current required for thermal transport is more complicated [12]

$$\mathbf{j}_Q = \sum_{\mathbf{q}} (\epsilon_{\mathbf{q}} - \mu) \mathbf{v}_{\mathbf{q}} c_{\mathbf{q}}^\dagger c_{\mathbf{q}} + \frac{U}{2} \sum_{\mathbf{q}, \mathbf{q}'} W(\mathbf{q} - \mathbf{q}') (\mathbf{v}_{\mathbf{q}} + \mathbf{v}_{\mathbf{q}'}) c_{\mathbf{q}}^\dagger c_{\mathbf{q}'} \quad (3)$$

with  $W(\mathbf{q}) = \frac{1}{N} \sum_j e^{-i\mathbf{q} \cdot \mathbf{R}_j} d_j^\dagger d_j$ , and thus the heat current contains both “kinetic” and “potential” terms. Quite generally, in terms of the Onsager co-efficients,  $L_{lm}(l, m = 1, 2)$  with  $L_{12} = L_{21}$ , one finds

$$\sigma_{dc}(T) = e^2 L_{11} \quad (4)$$

$$S_{el}(T) = -\frac{k_B}{e} \frac{L_{12}}{L_{11}} \quad (5)$$

and

$$K_{el}(T) = \frac{k_B^2}{T} \frac{L_{11} L_{22} - L_{12}^2}{L_{11}} \quad (6)$$

The  $L_{lm}$  can themselves be expressed in terms of the cluster propagators by noticing that these are the zero-frequency limit of the analytically continued “polarization” operators. Explicitly,  $L_{lm} = \lim_{\omega \rightarrow 0} \text{Re} \frac{i L_{lm}(\omega)}{\omega}$ , with

$$L_{11}(i\omega_n) = \int_0^\beta d\tau e^{i\omega_n \tau} \text{Tr} \frac{\langle T_\tau e^{-\beta H} j_e(\tau) j_e(0) \rangle}{Z} \quad (7)$$

$$L_{12}(i\omega_n) = L_{21}(i\omega_n) = \int_0^\beta d\tau e^{i\omega_n \tau} \text{Tr} \frac{\langle T_\tau e^{-\beta H} j_e(\tau) j_Q(0) \rangle}{Z} \quad (8)$$

and

$$L_{22}(i\omega_n) = \int_0^\beta d\tau e^{i\omega_n \tau} \text{Tr} \frac{\langle T_\tau e^{-\beta H} j_Q(\tau) j_Q(0) \rangle}{Z} \quad (9)$$

In absence of vertex corrections to transport co-efficients, the  $L_{lm}$  can finally be expressed in terms of the cluster propagators,  $G(\mathbf{K}, \omega)$ .  $L_{11}$  is the same as the one derived for the  $dc$  conductivity  $\sigma_{xx}(T)$  earlier [8]. The Onsager co-efficient relevant for heat transport is most conveniently given in the two-site cluster bonding-anti-bonding basis ( $S, P$  channels [14]) as the sum of the “kinetic” and “potential” contributions as sketched above,

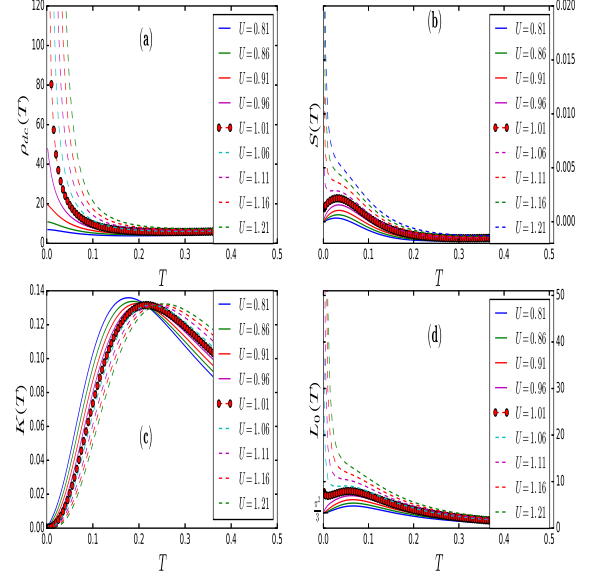


FIG. 4: (Color online) Results similar to those in Fig. 1 in main text, but now using single-site DMFT.

$L_{12} = L_{12}^k + L_{12}^p$ . and following Freericks *et al.* [10] for our two-site CDMFT, this reads

$$L_{12} = \sum_{a=S,P} \frac{T\sigma_0}{e^2} \int d\epsilon \rho_a(\epsilon) \int d\omega \left( -\frac{df(\omega)}{d\omega} \right) \omega A_a^2(\epsilon, \omega) \quad (10)$$

while  $L_{22}$  is given by

$$L_{22} = \sum_{a=S,P} \frac{T\sigma_0}{e^2} \int d\epsilon \rho_a(\epsilon) \int d\omega \left( -\frac{df(\omega)}{d\omega} \right) \omega^2 A_a^2(\epsilon, \omega) \quad (11)$$

Thus, thermal transport can be cleanly computed in our two-site CDMFT without any further approximation. This is because of the fortunate circumstance, namely that irreducible vertex corrections in the Bethe-Salpeter equations for all conductivities rigorously vanish in our cluster case as well, as pointed out in the main text. In the main text, we use the above equations to compute thermal transport in the FKM across the MIT.

## SI2: Single-Site DMFT Results for Thermal Transport

Here, we also use the same formalism to repeat the analysis of the main text using single-site DMFT results. Comparing with CDMFT results in the main text, several features stand out. These reveal very interesting differences between DMFT and CDMFT results, and we use these to propose that extensions of DMFT to include

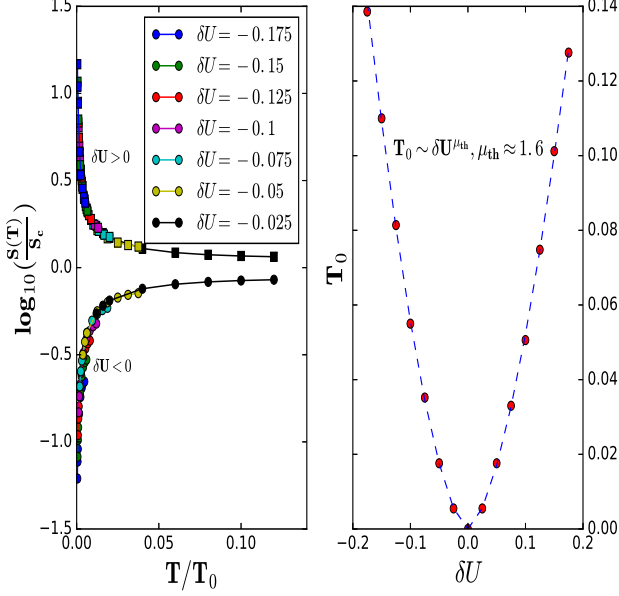


FIG. 5: (Color online) Results similar to those in Fig. 2 in main text, but now using single-site DMFT.

short-range spatial correlations seem to be *necessary* to discuss novel quantum critical scaling in thermal transport at the MIT.

We now show single-site DMFT results for electrical and thermal transport. In *dc* resistivity across the MIT, shown in Fig. 4 (which now occurs at a  $U_c^{DMFT} = 1.01$ ), we see features very similar to those found in CDMFT. However, (i)  $\rho_{dc}(T)$  at  $U_c$  now attains values  $O(40)\hbar/e^2$ , much smaller than the  $O(200)\hbar/e^2$  found in CDMFT. Correspondingly,  $S_{el}(T)$ ,  $K_{el}(T)$  and  $L_0(T)$  exhibit very similar behavior to that found in CDMFT, as shown in Fig. 4. At first sight, one may thus conclude that no qualitative difference exists between DMFT and CDMFT results.

However, closer inspection of DMFT results, obtained by performing the same scaling analysis as the one done in the main text, reveals crucial differences between DMFT and CDMFT results. Comparing scaling for  $S_{el}(T)$  within DMFT in Fig. 5 to those obtained from CDMFT in Fig. 2 in the main text reveals that (i) scaling holds over a much narrower window in DMFT compared with CDMFT, and (ii)  $\mu_{th}^{DMFT} = 1.6$ , compared to  $\mu_{th} = 1$  in CDMFT. It is thus more difficult to discern clean extended scaling behavior from DMFT results, and CDMFT clearly performs better in this respect. Moreover, repeating the analysis leading to Fig. 3 in the main text, we exhibit the results in Fig. 6. It is now clear that the scaling features in  $S_{el}(T)$ ,  $L_0(T)$ ,  $T^{-\nu}\sigma_{xx}(T)$  and

$T^{-1-\nu}K_{el}(T)$  are of much poorer quality than those obtained from two-site CDMFT results. The underlying reason for this inability of DMFT results to prop-

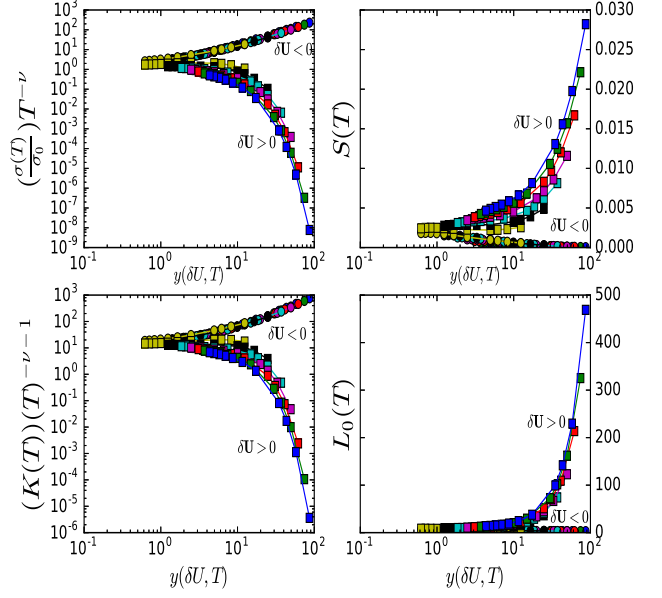


FIG. 6: (Color online) Results similar to those obtained in Fig. 3 in main text, but now using single-site DMFT.

erly describe quantum critical scaling of thermal transport can be understood heuristically as follows: in the main text, we have argued that thermal transport involves microscopic electronic processes associated with virtual hopping between a given site to its neighbors and back. Such second-order-in-hopping processes block charge transport, but allow energy transport, since such processes involve a gain of “super-exchange” (of Ising form for the FKM) energy. In single site DMFT, this process is  $O(1/d)$ , and so is not adequately captured. But precisely such a process *is* captured in our CDMFT, since the dynamical effects of inter-site (intracluster) correlations *are* fed back into CDMFT self-energies by construction [14].

Thus, while critical features in electrical transport may be adequately captured by single-site DMFT as above (though the critical exponents  $z$  and  $\nu$  are, as expected, different), we find that description of energy transport, and, in particular, much better elucidation of quantum critical thermal transport, requires cluster extensions capable of properly distinguishing between non-local aspects entering the distinct microscopic processes which underlie energy transport, as opposed to charge transport.